

Multigrid techniques for a divergence-free finite element discretization

S. TUREK*

Received June 20, 1994

Abstract — We derive basic properties for a class of discretely divergence-free finite elements which lead to a new proof of the smoothing property in a standard multigrid algorithm for solving the Stokes equations. Using appropriate grid transfer routines which are of second-order accuracy and interpolate in a divergence-free way, the ordinary multigrid convergence is obtained. The implementation of these operators is described in detail and the theoretical results are confirmed by numerical tests.

Keywords. Stokes equations, multigrid, discretely divergence-free finite elements.

1. INTRODUCTION

We consider multigrid techniques for solving the Stokes problem

$$\begin{aligned} -\Delta u + \nabla p &= f, \quad \nabla \cdot u = 0 \quad \text{in } \Omega \\ u &= g \quad \text{on } \partial\Omega \end{aligned} \tag{1.1}$$

where the pair $\{u, p\}$ represents the velocity and the pressure, respectively, of a viscous fluid contained in a bounded region $\Omega \subset \mathbb{R}^2$, with prescribed boundary values on $\partial\Omega$, and a given force f . We assume for simplicity that Ω is a convex polygon and the boundary values are homogeneous, $g = 0$. Using a standard weak discrete formulation of (1.1) and discretely divergence-free finite element subspaces $H_h^d \subset H_h$, we obtain a simplified positive definite scheme for the velocity only.

Find $u_h^d \in H_h^d$, such that

$$a_h(u_h^d, v_h^d) = (f, v_h^d) \quad \forall v_h^d \in H_h^d. \tag{1.2}$$

Here, H_h and the bilinear form $a_h(\cdot, \cdot)$ are discrete versions of $H_0^1(\Omega)$ and $(\nabla \cdot, \nabla \cdot)_{L^2}$, respectively, and are defined more precisely in the following section, where examples of these spaces and some of their basic properties are also given.

There are obvious advantages of explicitly constructing the subspaces H_h^d (eliminating the pressure, reducing the number of unknowns, definite stiffness matrices). However, a disadvantage is a complicated implementation and a bad condition number of the system matrices, which can be overcome by an appropriate multigrid algorithm with convergence rates independent of the mesh size. The theoretical problem is to prove the corresponding smoothing and approximation properties for the smoothing and grid transfer routines used. The convergence proof of the approximation property is similar to that of Brenner [2], while the smoothing property can be shown by a new technique, mainly using the basic properties of the finite element spaces. On the other hand,

*Institut für Angewandte Mathematik, University of Heidelberg, Germany

we have the practical problem of efficiently implementing these transfer operators. This can also be done by using a very precise and optimized code so that the final numerical effort of solving the Stokes equation is about the same as solving a scalar Poisson equation using the ordinary nonconforming spaces.

The subsequent numerical tests and the experience gathered in a fully developed nonsteady Navier-Stokes code for a wide range of Reynolds numbers [17] confirm the proposed theoretical results and show the high numerical flexibility of this class of finite elements.

$L^2(\Omega)$ and $H^m(\Omega)$ are the usual conventional Lebesgue and Sobolev spaces for the domain $\Omega \subset \mathbb{R}^2$ with the conventional norms $\|\cdot\|_0$ and $\|\cdot\|_m$. The inner product of $L^2(\Omega)$ is denoted by (\cdot, \cdot) . The space $H_0^1(\Omega)$ is the completion in $H^1(\Omega)$ of the space of test functions $C_0^\infty(\Omega)$ and $H^{-1}(\Omega)$ is its dual space. By $L_0^2(\Omega)$, we denote the subspace of all $L^2(\Omega)$ -functions over Ω having mean zero value. Vector valued functions and spaces and the corresponding norms and inner products are denoted as analogous scalar ones. We use a subscript h for discrete mesh-dependent constructions like triangulations, discrete spaces, norms, inner products, etc. Normal vectors are denoted by n , and tangential vectors by t ; $a \sim b$ implies that both expressions are equivalent, e.g. there are constants c_1, c_2 such that the relation $c_1 a \leq b \leq c_2 a$ is valid. Further special notation is introduced and described as needed.

2. THE SIMPLE NONCONFORMING FINITE ELEMENT SPACES

We consider the conventional steady Stokes problem (1.1) which reads with bilinear forms $a(u, v) := (\nabla u, \nabla v)$ and $b(p, v) := -(p, \nabla \cdot v)$:

Find a pair $\{u, p\} \in H_0^1(\Omega) \times L_0^2(\Omega)$, such that

$$a(u, v) + b(p, v) + b(q, u) = (f, v) \quad \forall \{v, q\} \in H_0^1(\Omega) \times L_0^2(\Omega). \quad (2.1)$$

An equivalent 'shorter' formulation with $V(\Omega) = \{v \in H_0^1(\Omega) : \nabla \cdot v = 0\}$ is:

Find $u \in V(\Omega)$, such that

$$a(u, v) = (f, v) \quad \forall v \in V(\Omega). \quad (2.2)$$

This problem has a unique solution for any force $f \in H^{-1}(\Omega)$ (see, e.g. [9]), which is a consequence of the familiar stability estimate

$$\sup_{v \in H_0^1(\Omega)} \frac{(q, \nabla \cdot v)}{\|\nabla v\|_0} \geq \beta \|q\|_0 > 0 \quad \forall q \in L_0^2(\Omega), \quad q \neq 0. \quad (2.3)$$

If $f \in L^2(\Omega)$, the solution is in $H^2(\Omega) \times H^1(\Omega)$ and satisfies the *a priori* estimate

$$\|u\|_2 + \|p\|_1 \leq c \|f\|_0. \quad (2.4)$$

For discretization, let T_h be a regular decomposition of the domain Ω into triangles or convex quadrilaterals denoted by T , where the mesh parameter $h > 0$ is the maximum diameter of the elements of T_h . By ∂T_h we denote the set of all boundary edges of elements $T \in T_h$. Besides, the family $\{T_h\}_h$ is assumed to satisfy the conventional uniform shape condition [6, 16]. The common edge between two elements $T_i, T_j \in T_h$ is denoted by Γ_{ij} with corresponding midpoint m_{ij} . Analogously, we define the boundary edges $\Gamma_{i,0} \subset (\partial T_h \cap \partial \Omega)$ with midpoints $m_{i,0}$. To obtain the fine mesh T_h from

a coarse mesh T_{2h} , we simply connect opposing midpoints (true domain boundaries are respected). In the new grid T_h coarse midpoints become vertices.

To approximate the problem (V) by the finite element method we introduce discrete spaces $H_h \approx H_0^1(\Omega)$ and $L_h \approx L_0^2(\Omega)$. For the (parametric) quadrilateral case we use the reference element $\hat{T} = [-1, 1]^2$ and define for each $T \in T_h$ the corresponding one-to-one-transformation $\psi_T: \hat{T} \rightarrow T$. Then we set ('rotated bilinear elements' [14])

$$\hat{Q}_1(T) := \{q \circ \psi_T^{-1} \mid q \in \text{span}\{x^2 - y^2, x, y, 1\}\} \quad (2.5)$$

while for the triangular case the linear functions from $P_1(T)$ are used. The degrees of freedom are determined by the nodal functionals $\{F_\Gamma^{(a/b)}(\cdot), \Gamma \subset \partial T_h\}$ with

$$F_\Gamma^{(a)}(v) := |\Gamma|^{-1} \oint_\Gamma v \, d\gamma \quad \text{or} \quad F_\Gamma^{(b)}(v) := v(m_\Gamma). \quad (2.6)$$

Either choice is unsolvable with $P_1(T)$ and $\hat{Q}_1(T)$, but for the quadrilateral case each of them leads to different finite element spaces since the applied midpoint rule is only correct for linear functions. Then, the corresponding (parametric) finite element spaces $H_h = H_h^{(a/b)}$ and L_h are defined as

$$L_h := \{q_h \in L_0^2(\Omega) \mid q_h|_T = \text{const} \quad \forall T \in T_h\}, \quad H_h^{(a/b)} := S_h^{(a/b)} \times S_h^{(a/b)} \quad (2.7)$$

$$S_h^{(a/b)} := \left\{ \begin{array}{l} v_h \in L^2(\Omega) \mid v_h|_T \in \hat{Q}_1(T) \quad \forall T \in T_h \\ v_h \text{ continuous w.r.t. all nodal functionals } F_{\Gamma_{ij}}^{(a/b)}(\cdot) \quad \forall \Gamma_{ij} \\ F_{\Gamma_{i0}}^{(a/b)}(v_h) = 0 \quad \forall \Gamma_{i0} \end{array} \right\}. \quad (2.8)$$

Our definitions lead to piecewise constant pressure approximations and edge-oriented velocity approximations with midpoints or integral mean values as degrees of freedom. Since the spaces $H_h^{(a/b)}$ are nonconforming, i.e., $H_h^{(a/b)} \not\subset H_0^1(\Omega)$, we have to deal with elementwise defined discrete bilinear forms and corresponding energy norms. We set

$$a_h(u_h, v_h) := \sum_{T \in T_h} \int_T \nabla u_h \cdot \nabla v_h \, dx, \quad \|v_h\|_h := a_h(v_h, v_h)^{1/2} \quad (2.9)$$

and define $b_h(\cdot, \cdot)$, dependent on the choice of $H_h^{(a/b)}$,

$$b_h(q_h, v_h) := - \sum_{T \in T_h} q_h|_T Q_T(v_h), \quad Q_T(v_h) := \sum_{\Gamma \subset \partial T} |\Gamma| F_\Gamma^{(a/b)}(v_h) \cdot n_\Gamma \quad (2.10)$$

which leads for $H_h^{(b)}$ to an additional $O(h^2)$ quadrature error. Furthermore, let $j_h: L_0^2(\Omega) \rightarrow L_h$ be the operator of piecewise constant interpolation (modified to retain the zero-mean value property) which satisfies for $q \in L_0^2(\Omega) \cap H^1(\Omega)$ [16]

$$\|q - j_h q\|_0 \leq ch \|q\|_1 \quad \forall q \in L_0^2(\Omega) \cap H^1(\Omega) \quad (2.11)$$

and let $i_h^{(a/b)}: H_0^1(\Omega) \rightarrow H_h^{(a/b)}$ be the global interpolation operator in $H_h^{(a/b)}$

$$F_\Gamma(i_h^{(a/b)} v) = F_\Gamma(v) \quad \forall \Gamma \subset \partial T_h. \quad (2.12)$$

Using additional regularity assumptions on the mesh in the quadrilateral case [14, 16], we can state:

Lemma 2.1. *For the interpolation operators $i_h = i_h^{(a/b)}$:*

$$\|v - i_h v\|_0 + h \|v - i_h v\|_h \leq ch^2 \|v\|_2 \quad \forall v \in H_0^1(\Omega) \cap H^2(\Omega).$$

Analogously, we can show [14, 16] that for the element pairs $(H_h^{(a/b)}, L_h)$ the discrete version of the continuous estimate (2.3) is valid:

$$\tilde{\beta} \|p_h\|_0 \leq \max_{v_h \in H_h^{(a/b)}} \frac{b_h(p_h, v_h)}{\|v_h\|_h} \quad (2.13)$$

and we can essentially end up with the asymptotic error estimate [14, 16]:

Lemma 2.2. *Suppose that the preceding assumptions are valid. Then, the discrete Stokes problems have unique solutions $\{u_h, p_h\} \in H_h^{(a/b)} \times L_h$, and the inequality holds:*

$$\|u - u_h\|_0 + h \|u - u_h\|_h + h \|p - p_h\|_0 \leq ch^2 \{\|u\|_2 + \|p\|_1\}. \quad (2.14)$$

To explicitly construct the divergence-free subspaces $H_h^d \subset H_h$ we give the definition.

Definition 2.1. *A function $v_h \in H_h$ is called a discretely divergence-free function, if*

$$b_h(q_h, v_h) = 0 \quad \forall q_h \in L_h. \quad (2.15)$$

Since only piecewise constant pressure approximations are used, an equivalent criterion is

$$Q_T(v_h) = 0 \quad \forall T \in T_h. \quad (2.16)$$

With these modifications we can introduce subspaces $H_h^d \subset H_h$, and our discrete problem for the velocity is reduced to:

Find $u_h^d \in H_h^d$, such that

$$a_h(u_h^d, v_h^d) = (f, v_h^d) \quad \forall v_h^d \in H_h^d. \quad (2.17)$$

Finally, the corresponding pressure $p_h \in L_h$ is determined by the condition

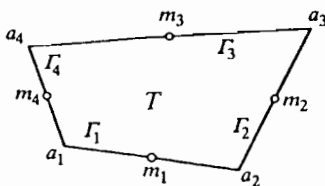
$$b_h(p_h, v_h^r) = (f, v_h^r) - a_h(u_h^d, v_h^r) \quad \forall v_h^r \in H_h^r \quad (2.18)$$

where the functions v_h^r span the curl-free part of the complete space H_h . In our configuration this is done (Section 3) by a marching process from element to element not solving any linear system of equations. In the end we obtain the same error estimates for u_h^d and p_h as in Lemma 2.1.

3. THE DIVERGENCE-FREE SUBSPACES AND THEIR PROPERTIES

Divergence-free subspaces have originally been introduced and analyzed in [7] and [9]. Some helpful analytical results may be found in [8]. We show the construction process and some properties, which are important for a better understanding, and the multigrid proofs.

We consider a general quadrilateral $T \in T_h$ (Fig. 1) with vertices a^i , midpoints m^j , edges Γ^j , unit tangential vectors t^j , and normal unit vectors n^j . Let $\varphi_h^j \in S_h^{(a/b)}$ be

Figure 1. General quadrilateral T .

ordinary nodal basis functions in the finite element space $S_h = S_h^{(a/b)}$, restricted to element T , satisfying $F_{\Gamma}(\varphi_h^j) = \delta_{ij}$, $i, j = 1, \dots, 4$. Then, the first group of trial functions $\{v_h^{i,t}\}$ of H_h^d corresponding to the edges of T_h is given by the local definition

$$v_h^{i,t} \in \{\varphi_h^j t^j, j = 1, \dots, 4\}. \quad (3.1)$$

The second group $\{v_h^{i,\psi}\}$ corresponding to the vertices is locally determined by

$$v_h^{i,\psi} \in \left\{ \frac{\varphi_h^k n^k}{|\Gamma^k|} - \frac{\varphi_h^j n^j}{|\Gamma^j|}, \quad j = 1, \dots, 4, \quad k = (j + 2) \bmod 4 + 1 \right\}. \quad (3.2)$$

Thus, we get approximations for the tangential velocities at the edges, and for the streamfunction values at the nodes (see also [10]). The full space H_h^d is the direct sum of these two subspaces. When defining the inner product $(\cdot, \cdot)_{d,h}$ on H_h^d by

$$(u_h, v_h)_{d,h} := \frac{1}{4} \sum_{T \in T_h} |T| \sum_{\Gamma \in \partial T} F_{\Gamma}(u_h) \cdot F_{\Gamma}(v_h) \quad (3.3)$$

the induced norm $\|\cdot\|_{d,h}$ is equivalent to the L^2 -norm (or even identical for the triangular case with weight $1/3$), and both groups of trial functions are orthogonal relative to this form. If we eliminate one of the functions $\{v_h^{i,\psi}\}$ by prescribing the stream function value at one (boundary) point or requiring that the mean value be zero, we get a basis for the discretely divergence-free subspace H_h^d , assuming that our problem has only one boundary component. This is a simple consequence of the familiar Euler–Poincaré characteristic.

Lemma 3.1 (Euler–Poincaré characteristic). *Define for a triangulation T_h :*

$$NVT := \# \text{vertices of } T_h$$

$$NMT := \# \text{midpoints of } T_h (= \# \text{edges of } T_h)$$

$$NEL := \# \text{elements of } T_h$$

$$NBC := \# \text{boundary components of } \partial \Omega$$

then the formula holds:

$$NVT + NEL + NBC = NMT + 2.$$

For only one boundary component, $NBC = 1$, the dimension of the subspace H_h^d must be

$$2 \cdot NMT - NEL = NMT - NEL + NVT + NEL - 1 = NMT + NVT - 1.$$

By construction, we have $NMT + NVT$ trial functions, which implies that at least one of them has to be eliminated. It is easy to see that the tangential functions of (3.1) are orthogonal relative to $\|\cdot\|_{d,h}$. For the remaining functions $v_h^\psi = \sum \Psi^i v_h^{i,\psi}$, we can show

$$\|v_h^\psi\|_{d,h}^2 \sim \sum_{T \in \mathcal{T}_h} |T| \sum_{\Gamma^j \in \partial T} \frac{|\Psi^{j+1} - \Psi^j|^2}{|\Gamma^j|^2} \sim \sum_{T \in \mathcal{T}_h} \sum_{k=1}^4 |\Psi^{k+1} - \Psi^k|^2. \quad (3.4)$$

This implies that the mass matrix is spectrally equivalent to the stiffness matrix corresponding to the discretization of the Poisson equation with natural boundary conditions for conforming linear or bilinear elements. Therefore, eliminating one of these functions leads to a basis in two space dimensions, at least for the case of one boundary component.

After introducing these new basis functions the size of our linear system for the quadrilateral case is reduced from about $5NVT$ unknowns for the ordinary formulation to approximately $3NVT$ for the divergence-free case, and from $8NVT$ to about $4NVT$ for the triangular case.

Let $v_h \in H_h^d$ be a discretely divergence-free function with the two different representations

$$v_h = \sum_i \Psi^i v_h^{i,\psi} + \sum_j U_t^j v_h^{j,t} = \sum_k U^k \varphi_h^k + \sum_l V^l \varphi_h^l \quad (3.5)$$

where Ψ , U_t are the coefficient vectors in a divergence-free and U , V in a primitive representation. Then, we can construct [8] rectangular transfer matrices R_p^d and R_d^p , such that

$$R_p^d \begin{bmatrix} U \\ V \end{bmatrix} = \begin{bmatrix} \Psi \\ U_t \end{bmatrix}, \quad R_d^p \begin{bmatrix} \Psi \\ U_t \end{bmatrix} = \begin{bmatrix} U \\ V \end{bmatrix}. \quad (3.6)$$

Rewriting $v_h \in H_h^d$ as

$$\begin{aligned} v_h &= \sum_i X^{d,i} v_h^{i,d} = \sum_j \Psi^j (h \cdot v_h^{j,\psi}) + \sum_k U_t^k v_h^{k,t} \\ &= \sum_l X^{p,l} v_h^{l,p} = \sum_m U^{p,m} \varphi_h^{m,p} + \sum_l V^{p,l} \varphi_h^{l,p} \end{aligned} \quad (3.7)$$

with coefficient vectors X^d and X^p , we obtain

$$R_p^d R_d^p X^d = X^d, \quad R_d^p R_p^d X^p = X^p. \quad (3.8)$$

Furthermore, let S_h^l be ordinary conforming linear or bilinear finite element spaces with nodal basis φ_h^l , satisfying $\varphi_h^{j,l}(a_i) = \delta_{ij}$ for all vertices a_i of T_h . By S_l we denote the corresponding positive definite stiffness matrix. Analogously, we assume that S_p denotes the corresponding stiffness matrix for the scalar nonconforming basis functions,

$$S_l^{(i,j)} = \sum_{T \in \mathcal{T}_h} \int_T \nabla \varphi_h^{i,l} \cdot \nabla \varphi_h^{j,l} dx, \quad S_p^{(i,j)} = \sum_{T \in \mathcal{T}_h} \int_T \nabla \varphi_h^{i,p} \cdot \nabla \varphi_h^{j,p} dx$$

and define

$$S_{lp} := \begin{bmatrix} S_l & 0 \\ 0 & S_p \end{bmatrix}, \quad Q_d := \begin{bmatrix} S_l^{1/2} & 0 \\ 0 & I_p \end{bmatrix} \quad (3.9)$$

The corresponding details are straightforward but very technical, therefore, we omit them. Then, by the previous corollary we end up with

$$|||\tilde{S}_p^{1/2} R_d^p Q_d^{-1} S_{lp}^{-1/2}|||_0 \leq c. \quad (3.14)$$

We can write the second expression as

$$|||S_{lp}^{1/2} Q_d X^d|||_0^2 = (X^d)^T \begin{bmatrix} S_l S_l & 0 \\ 0 & S_p \end{bmatrix} X^d \quad (3.15)$$

and obtain with the basic eigenvalue estimates for standard finite element discretizations

$$|||v_h|||_1^2 \leq c(\Psi^T S_l S_l \Psi + U_t^T S_p U_t) \leq c(\Psi^T S_l S_l \Psi + U_t^T U_t). \quad (3.16)$$

By definition we also know

$$|||v_h|||_0^2 = \Psi^T \Psi + U_t^T U_t. \quad (3.17)$$

Then, a first result in matrix-vector notation reads

$$|||v_h|||_s^2 \leq c \begin{bmatrix} \Psi \\ U_t \end{bmatrix}^T \begin{bmatrix} S_l S_l & 0 \\ 0 & I_p \end{bmatrix}^s \begin{bmatrix} \Psi \\ U_t \end{bmatrix} \quad (3.18)$$

and using interpolation arguments for norm scales (compare, for instance, with [13]), we obtain for $s = 1/2$

$$|||v_h|||_{1/2}^2 \leq c(\Psi^T S_l \Psi + U_t^T U_t) = c|||Q_d X^d|||_0^2. \quad (3.19)$$

By Corollary 3.1 we finally get:

$$|||v_h|||_{1/2} \leq ch^{-1} |||v_h|||_0. \quad \blacksquare$$

We also need estimates for the condition numbers of mass and stiffness matrices. As before we may rewrite $v_h \in H_h^d$ as

$$v_h = \sum_i X^{d,i} v_h^{i,d} = \sum_j \Psi^j(h \cdot v_h^{j,\psi}) + \sum_k U_t^k v_h^{k,t}.$$

Using the standard finite element estimates

$$|||v_h|||_0 \leq c |||v_h|||_h \leq ch^{-1} |||v_h|||_0 \quad (3.20)$$

we obtain for the L_2 - and energy norm

$$\begin{aligned} |||v_h|||_1^2 &= |||v_h|||_h^2 \leq ch^{-2} |||v_h|||_0^2 \leq c |||Q_d X^d|||_E^2 = c(\Psi^T S_l \Psi + U_t^T U_t) \\ &\leq c(\Psi^T \Psi + U_t^T U_t) = c |||v_h|||_0^2 \end{aligned} \quad (3.21)$$

$$\begin{aligned} |||v_h|||_0^2 &= \Psi^T \Psi + U_t^T U_t \leq c(h^{-2} \Psi^T S_l \Psi + U_t^T U_t) \\ &\leq ch^{-2} (\Psi^T S_l \Psi + U_t^T U_t) = ch^{-2} |||Q_d X^d|||_E^2 \\ &\leq ch^{-4} |||v_h|||_0^2 \leq ch^{-4} |||v_h|||_h^2 = ch^{-4} |||v_h|||_1^2. \end{aligned} \quad (3.22)$$

We summarize these results in the lemma.

Lemma 3.3. For functions $v_h \in H_h^d$, there holds:

(1) The condition number of the mass matrix M_d is $O(h^{-2})$; that is

$$ch^4 |||v_h|||_0 \leq \|v_h\|_0^2 \leq Ch^2 |||v_h|||_0^2.$$

(2) The condition number of the stiffness matrix S_d is $O(h^{-4})$; that is

$$ch^4 |||v_h|||_0^2 \leq |||v_h|||_1^2 \leq C |||v_h|||_0^2.$$

In the rest of this section we want to elucidate practical questions concerning the problem of several boundary components and the calculation of the pressure. We are mainly interested in flows associated with the boundary conditions

$$g \cdot n|_{\Gamma_i} = 0, \quad i = 2, 3, \dots, n \quad (3.23)$$

on each additional boundary component $\{\Gamma_i, i = 2, 3, \dots, n\}$. For such boundary conditions we know that the streamfunction takes the fixed but unknown value c_i on Γ_i . In connection with iterative solution techniques for the finite elements used we apply a so-called projection method [8]. This implies that before and after each matrix-vector multiplication we have to correct the boundary values. We calculate the mean value of the streamfunction values on each boundary component Γ_i , and prescribe this value as a new guess to c_i . This method works for any number of components without modifying the code by explicitly constructing the corresponding nonlocal basis functions (see [15]).

In order to calculate $p_h \in L_h$ corresponding to the already known velocity $u_h^d \in H_h^d$, we use the remaining part of discretely curl-free trial functions $H_h^r \subset H_h$:

$$b_h(p_h, v_h^r) = (f, v_h^r) - a_h(u_h^d, v_h^r) \quad \forall v_h^r \in H_h^r. \quad (3.24)$$

Analogous to our tangential trial functions $v_h^{i,t}$, we construct locally normal functions $v_h^{i,n}$,

$$v_{h|T}^{i,n} \in \{\varphi_h^j n^j, j = 1, \dots, 4\} \quad (3.25)$$

which have support on only two elements called T_1 and T_2 with common edge Γ . Using them, equation (3.24) is reduced to

$$p_{h|T_1} Q_{T_1}(v_h^{i,n}) + p_{h|T_2} Q_{T_2}(v_h^{i,n}) = (f, v_h^{i,n}) - a_h(u_h^d, v_h^{i,n}) \quad (3.26)$$

which can be further simplified

$$\begin{aligned} p_{h|T_1} Q_{T_1}(v_h^{i,n}) + p_{h|T_2} Q_{T_2}(v_h^{i,n}) &= p_{h|T_1} |\Gamma| F_\Gamma(v_h^{i,n}) \cdot n_i - p_{h|T_2} |\Gamma| F_\Gamma(v_h^{i,n}) \cdot n_i \\ &= |\Gamma| (p_{h|T_1} - p_{h|T_2}). \end{aligned} \quad (3.27)$$

Fixing the pressure value in one element, the other values can be calculated by a marching process not solving any linear system of equations.

To conclude, we would like to state the advantages of the discretely divergence-free finite element spaces. The pressure is decoupled from the velocity, which results in a reduction of the unknowns and leading to definite systems of equations. The pressure can be obtained from the velocity not solving a linear system. Another advantage is that for graphical postprocessing the streamfunction values are directly available. Of course,

this requires a greater computational effort. As we pointed out, this is mainly due to constructing the basis functions and increasing the condition numbers. A remedy for this trouble is the multigrid algorithm.

4. THE MULTIGRID ALGORITHM AND ITS ANALYSIS

The following algorithm and its analysis follow the ideas of Brenner [2-4]. Any differences from Brenner's approach are pointed out in the text.

Let $\{T_{h_l}\}_{h_l}$ be a family of regular subdivisions which are obtained by the refinement process discussed in Section 2. The discrete Stokes problem at level k reads:

Find $u_k^d \in H_k^d$, such that

$$a_k(u_k^d, v_k^d) = (f, v_k^d) \quad \forall v_k^d \in H_k^d. \quad (4.1)$$

As before, we write $v_k \in H_k^d$ as

$$v_k = \sum_i X^{d,i} v_k^{i,d} = \sum_j \Psi^j(h_k \cdot v_k^{j,\psi}) + \sum_l U_l^i v_k^{i,l} \quad (4.2)$$

and introduce the discrete scalar product $(\cdot, \cdot)_k$

$$(v_k, w_k)_k := \sum_i \Psi_v^i \Psi_w^i + \sum_j U_{i,v}^j U_{i,w}^j. \quad (4.3)$$

This corresponds to the Euclidean scalar product $\langle \cdot, \cdot \rangle_E$, since

$$(v_k, w_k)_k = \langle X_v^d, X_w^d \rangle_E. \quad (4.4)$$

The prolongation operator $I_{k-1}^k: H_{k-1}^d \rightarrow H_k^d$ and its adjoint restriction operator $I_k^{k-1}: H_k^d \rightarrow H_{k-1}^d$ are defined by

$$(I_{k-1}^{k-1} w_k, v_{k-1})_{k-1} = (w_k, I_{k-1}^k v_{k-1})_k \quad \forall v_{k-1} \in H_{k-1}^d, \quad \forall w_k \in H_k^d. \quad (4.5)$$

We further define the positive definite discrete operator $A_k: H_k^d \rightarrow H_k^d$

$$(A_k v_k, w_k)_k = a_k(v_k, w_k) \quad \forall v_k, w_k \in H_k^d \quad (4.6)$$

so that the eigenvalues λ_k^i of A_k satisfy (compare with Lemma 3.3)

$$O(h_k^4) \leq \lambda_k^i \leq \dots \leq \lambda_k^{max} \leq c \quad (4.7)$$

where c is a constant independent of h_k . Finally, we introduce the operator $P_k^{k-1}: H_k^d \rightarrow H_{k-1}^d$, which is the adjoint of I_{k-1}^k relative to $a_k(\cdot, \cdot)$,

$$a_{k-1}(P_k^{k-1} w_k, v_{k-1}) = a_k(w_k, I_{k-1}^k v_{k-1}) \quad \forall v_{k-1} \in H_{k-1}^d, \quad \forall w_k \in H_k^d. \quad (4.8)$$

Corollary 4.1. *With the above definitions the inequality holds: $P_k^{k-1} = A_{k-1}^{-1} I_{k-1}^{k-1} A_k$.*

Again we introduce the mesh-dependent norm scale $||| \cdot |||_{s,k}$ on H_k^d

$$|||v_k|||_{s,k} := (A_k^s v_k, v_k)_k^{1/2} \quad (4.9)$$

and repeat the estimates from the preceding section

$$|||v_k|||_1^2 = \|v_k\|_k^2, \quad |||v_k|||_0^2 = \|X_v^d\|_E^2, \quad |||v_k|||_{1/2}^2 \leq ch_k^{-2} \|v_k\|_0^2. \quad (4.10)$$

Our k -level multigrid algorithm $MG(k, \cdot, \cdot)$ for solving the problem (V_k^d) reads:

The k -level iteration $MG(k, u_k^0, g_k)$

The k -level iteration with initial guess u_k^0 yields an approximation to u_k , the solution to the problem

$$A_k u_k = g_k. \quad (4.11)$$

One step can be described in the following way:

For $k = 1$, $MG(1, u_1^0, g_1)$ is the exact solution: $MG(1, u_1^0, g_1) = A_1^{-1} g_1$.

For $k > 1$, there are four steps:

(1) m -Presmoothing steps.

Apply m smoothing steps to u_k^0 to obtain u_k^m .

For the damped Jacobi method this procedure reads: Let u_k^l , $l = 1, \dots, m$, be defined recursively by the equations

$$u_k^l = u_k^{l-1} + \omega_k (g_k - A_k u_k^{l-1}) \quad (4.12)$$

where ω_k is a damping parameter which has to be smaller than the inverse of the largest eigenvalue λ_k^{\max} .

(2) A correction step.

Calculate the restricted defect

$$g_{k-1} = I_k^{k-1} (g_k - A_k u_k^m) \quad (4.13)$$

and let $u_{k-1}^i \in H_{k-1}^d$, $1 \leq i \leq p$, $p \geq 2$, be defined recursively by

$$u_{k-1}^i = MG(k-1, u_{k-1}^{i-1}, g_{k-1}), \quad 1 \leq i \leq p, \quad u_{k-1}^0 = 0. \quad (4.14)$$

(3) Step size control.

Calculate u_k^{m+1} by

$$u_k^{m+1} = u_k^m + \alpha_k I_{k-1}^k u_{k-1}^p \quad (4.15)$$

where the parameter α_k may be a fixed or chosen adaptively chosen value so as to minimize the error $u_k^{m+1} - u_k$ in the energy norm, that is

$$\alpha_k = \frac{(g_k - A_k u_k^m, I_{k-1}^k u_{k-1}^p)_k}{(A_k I_{k-1}^k u_{k-1}^p, I_{k-1}^k u_{k-1}^p)_k}. \quad (4.16)$$

(4) m -Postsmoothing steps.

Analogous to step (1), apply m smoothing steps to u_k^{m+1} to obtain u_k^{2m+1} .

One iteration step $MG(k, \cdot, \cdot)$ yields, given an initial u_k^0 , the new approximate u_k^{2m+1} , which may be written as

$$MG(k, u_k^0, g_k) = u_k^{2m+1}. \quad (4.17)$$

The full multigrid algorithm with optimal efficiency [$O(n_k)$ arithmetic operations] consists of a nested iteration of this scheme. For practical applications other smoothing

schemes like Gauß-Seidel or ILU may be used and the number of pre- and postsmoothing steps may vary. Also, other cycle-types like the V-cycle ($p = 1$) or our favourite the F-cycle [16] may be taken.

For the convergence analysis, we restrict ourselves to the case of a two-level method ($k = 2$) without postsmoothing and step length control and show the ordinary smoothing and approximation property for the damped Jacobi-method. The essential new approach is that the smoothing property may be shown using only the properties of the finite element spaces. This is in contrast to the work of Brenner [2], where a strong relation between triangular divergence-free finite elements and the nonconforming Morley element was used.

Lemma 4.1 (Smoothing property). *For the error $e_h^m := u_h - u_h^m$ the relations hold for $\rho(m) = m^{-1/4}$:*

$$(a) \quad |||e_h^m|||_1 \leq c\rho(m)h^{-1}\|e_h^0\|_0$$

$$(b) \quad |||e_h^m|||_{3/2} \leq c\rho(m)^2h^{-1}\|e_h^0\|_0.$$

Proof. Applying m damped Jacobi-steps to e_h^0 yields

$$e_h^m = (I_h - \omega_h A_h)^m e_h^0. \quad (4.18)$$

Furthermore,

$$\begin{aligned} A_h^{1/2} e_h^m &= A_h^{1/2} (I_h - \omega_h A_h)^m e_h^0 \\ &= \omega_h^{-1/4} A_h^{1/4} \omega_h^{1/4} A_h^{1/4} (I_h - \omega_h A_h)^m A_h^{-1/4} A_h^{1/4} e_h^0 \end{aligned}$$

and hence

$$\begin{aligned} |||A_h^{1/2} e_h^m|||_0^2 &\leq \omega_h^{-1/2} |||A_h^{1/4} \omega_h^{1/4} A_h^{1/4} (I_h - \omega_h A_h)^m A_h^{-1/4}|||_0^2 |||A_h^{1/4} e_h^0|||_0^2 \\ &\leq c |||(\omega_h A_h)^{1/4} (I_h - \omega_h A_h)^m|||_0^2 |||A_h^{1/4} e_h^0|||_0^2 \end{aligned}$$

respectively,

$$|||e_h^m|||_1^2 \leq c |||(\omega_h A_h)^{1/4} (I_h - \omega_h A_h)^m|||_0^2 |||e_h^0|||_{1/2}^2. \quad (4.19)$$

By standard arguments for positive definite operators (see, e.g. [1, 11])

$$|||(\omega_h A_h)^{1/4} (I_h - \omega_h A_h)^m|||_0 \leq cm^{-1/4} = c\rho(m) \quad (4.20)$$

and, therefore, with the help of Lemma 3.2,

$$|||e_h^m|||_1 \leq c\rho(m) |||e_h^0|||_{1/2} \leq c\rho(m)h^{-1}\|e_h^0\|_0.$$

Analogously, for $s = 3/2$, we have

$$A_h^{3/4} e_h^m = A_h^{3/4} (I_h - \omega_h A_h)^m e_h^0 = \omega_h^{-1/2} A_h^{1/4} \omega_h^{1/2} A_h^{1/2} (I_h - \omega_h A_h)^m A_h^{-1/4} A_h^{1/4} e_h^0 \quad (4.21)$$

resulting in:

$$|||e_h^m|||_{3/2} \leq c\rho(m)^2h^{-1}\|e_h^0\|_0. \quad \blacksquare \quad (4.22)$$

The main work was done in the preceding section by proving Lemma 3.2. We now show the appropriate approximation property following the ideas of Brenner [2-4]. The

main difference is that the quadrilateral case is evaluated without using explicitly the fact that the finite elements are divergence-free in a pointwise sense.

Since in the 2-level iteration the correction equation is solved exactly, the coarse grid solution $u_{2h} := u_{2h}^p$ satisfies:

$$u_{2h} = A_{2h}^{-1} g_{2h} = A_{2h}^{-1} [I_h^{2h} (g_h - A_h u_h^m)] = A_{2h}^{-1} I_h^{2h} A_h e_h^m = P_h^{2h} e_h^m. \quad (4.23)$$

We make the following assumptions concerning the prolongation operator:

Condition I.

- (1) $\|I_{2h}^h v_{2h} - v_{2h}\|_0 \leq ch \|v_{2h}\|_{2h} \quad \forall v_{2h} \in H_{2h}^d$;
- (2) $\exists \Pi_{h/2h}: V(\Omega) \cap H^2(\Omega) \rightarrow H_{h/2h}^d$, such that

$$\|v - \Pi_{h/2h} v\|_0 + h \|v - \Pi_{h/2h} v\|_{h/2h} \leq c_1 h^2 \|v\|_2 \quad \forall v \in V(\Omega) \cap H^2(\Omega)$$

$$\|\Pi_h v - I_{2h}^h \Pi_{2h} v\|_0 + h \|\Pi_h v - I_{2h}^h \Pi_{2h} v\|_h \leq ch^2 \|v\|_2 \quad \forall v \in V(\Omega) \cap H^2(\Omega).$$

Condition II.

- (1) $(I_{2h}^h w_{2h} - w_{2h}, v_h) = 0 \quad \forall w_{2h} \in H_{2h}^d \quad \forall v_h \in H_h^d$;
- (2) $\|A_{2h}^{-1/4} I_h^{2h} A_h^{1/4} v_h\|_0 \leq c \|v_h\|_0 \quad \forall v_h \in H_h^d$.

Condition II is satisfied by the L_2 -projection only. Furthermore, condition I and the inverse estimate for finite elements imply the relations:

Corollary 4.2. For $v_{2h} \in H_{2h}^d$: $\|I_{2h}^h v_{2h}\|_h \leq c \|v_{2h}\|_{2h}$, $\|I_{2h}^h v_{2h}\|_0 \leq c \|v_{2h}\|_0$.

Corollary 4.3. For $v_h \in H_h^d$: $\|P_h^{2h} v_h\|_{2h} \leq c \|v_h\|_h$.

We can now show the main result for the approximation property.

Lemma 4.2 (Approximation property). For $v_h \in H_h^d$ and $\hat{v}_h = (I_h - I_{2h}^h P_h^{2h}) v_h \in H_h^d$: $\|\hat{v}_h\|_0 \leq ch \|\hat{v}_h\|_1$. If Condition II is valid, then: $\|\hat{v}_h\|_0 \leq ch \|\hat{v}_h\|_{3/2}$.

Proof. Let $v_h \in H_h^d$ and $\hat{v}_h = (I_h - I_{2h}^h P_h^{2h}) v_h \in H_h^d$ be given. We consider the auxiliary problem:

Find $r \in V(\Omega)$, such that

$$a(r, w) = (\hat{v}_h, w) \quad \forall w \in V(\Omega). \quad (4.24)$$

We already know from the *a priori* estimate (2.4) that

$$\|r\|_2 \leq c \|\hat{v}_h\|_0. \quad (4.25)$$

Let $r_h \in H_h^d$ and $r_{2h} \in H_{2h}^d$ be the corresponding discrete solutions which satisfy the error estimates

$$\|r - r_h\|_0 + h \|r - r_h\|_h \leq ch^2 \|\hat{v}_h\|_0$$

$$\|r - r_{2h}\|_0 + h \|r - r_{2h}\|_{2h} \leq Ch^2 \|\hat{v}_h\|_0. \quad (4.26)$$

Introducing the term $z_{2h} = P_h^{2h} v_h$, we can write

$$\begin{aligned} (\hat{v}_h, \hat{v}_h) &= (\hat{v}_h, v_h - I_{2h}^h z_{2h}) \\ &= a_h(r_h, v_h) - (\hat{v}_h, I_{2h}^h z_{2h} - z_{2h}) - (\hat{v}_h, z_{2h}) \\ &= a_h(r_h, v_h) - a_{2h}(r_{2h}, z_{2h}) - (\hat{v}_h, I_{2h}^h z_{2h} - z_{2h}). \end{aligned}$$

Further, letting $\Pi_h: V(\Omega) \cap H^2(\Omega) \rightarrow H_h^d$ and $\Pi_{2h}: V(\Omega) \cap H^2(\Omega) \rightarrow H_{2h}^d$ be interpolation operators as in Condition I, we have

$$\begin{aligned} \|\hat{v}_h\|_0^2 &= a_h(r_h - \Pi_h r, v_h) - a_{2h}(r_{2h} - \Pi_{2h} r, z_{2h}) \\ &\quad + a_h(\Pi_h r, v_h) - a_{2h}(\Pi_{2h} r, z_{2h}) - (\hat{v}_h, I_{2h}^h z_{2h} - z_{2h}) \\ &= a_h(r_h - \Pi_h r, v_h) - a_{2h}(r_{2h} - \Pi_{2h} r, z_{2h}) \\ &\quad + a_h(\Pi_h r - I_{2h}^h \Pi_{2h} r, v_h) - (\hat{v}_h, I_{2h}^h z_{2h} - z_{2h}) \\ &= \Sigma_1 + \Sigma_2 + \Sigma_3 + \Sigma_4. \end{aligned}$$

We now show that each term Σ_i can be estimated by

$$|\Sigma_i| \leq ch \|v_h\|_1 \|\hat{v}_h\|_0, \quad \text{respectively,} \quad |\Sigma_i| \leq ch \|v_h\|_{3/2} \|\hat{v}_h\|_0$$

which are valid because

$$\begin{aligned} |\Sigma_1| &= |a_h(r_h - \Pi_h r, v_h)| \leq \|r_h - \Pi_h r\|_h \|v_h\|_h \leq ch \|\hat{v}_h\|_0 \|v_h\|_h \\ |\Sigma_2| &= |a_{2h}(r_{2h} - \Pi_{2h} r, z_{2h})| \leq \|r_{2h} - \Pi_{2h} r\|_{2h} \|P_h^{2h} v_h\|_{2h} \leq ch \|\hat{v}_h\|_0 \|v_h\|_h \\ |\Sigma_3| &= |a_h(\Pi_h r - I_{2h}^h \Pi_{2h} r, v_h)| \leq \|\Pi_h r - I_{2h}^h \Pi_{2h} r\|_h \|v_h\|_h \leq ch \|\hat{v}_h\|_0 \|v_h\|_h \\ |\Sigma_4| &= |(\hat{v}_h, I_{2h}^h z_{2h} - z_{2h})| \leq \|\hat{v}_h\|_0 \|I_{2h}^h z_{2h} - z_{2h}\|_0 \\ &\leq ch \|\hat{v}_h\|_0 \|P_h^{2h} v_h\|_{2h} \leq ch \|\hat{v}_h\|_0 \|v_h\|_h. \end{aligned}$$

As a result, we immediately obtain: $\|\hat{v}_h\|_0 \leq ch \|v_h\|_1$.

For $s = 3/2$, we also require Condition II:

$$\begin{aligned} |\Sigma_1| &\leq \|r_h - \Pi_h r\|_{1/2} \|v_h\|_{3/2} \\ &\leq ch^{-1} \|r_h - \Pi_h r\|_0 \|v_h\|_{3/2} \leq ch \|\hat{v}_h\|_0 \|v_h\|_{3/2} \\ |\Sigma_2| &\leq \|r_{2h} - \Pi_{2h} r\|_{1/2} \|P_h^{2h} v_h\|_{3/2} \\ &\leq ch^{-1} \|r_{2h} - \Pi_{2h} r\|_0 \|A_{2h}^{3/4} A_{2h}^{-1} I_{2h}^{2h} A_h v_h\|_0 \\ &\leq ch \|\hat{v}_h\|_0 \|A_{2h}^{-1/4} I_{2h}^{2h} A_h^{1/4} A_h^{3/4} v_h\|_0 \leq ch \|\hat{v}_h\|_0 \|v_h\|_{3/2} \\ |\Sigma_3| &\leq \|\Pi_h r - I_{2h}^h \Pi_{2h} r\|_{1/2} \|v_h\|_{3/2} \leq ch^{-1} \|\Pi_h r - I_{2h}^h \Pi_{2h} r_{2h}\|_0 \|v_h\|_{3/2} \\ &\leq ch \|\hat{v}_h\|_0 \|v_h\|_{3/2} \\ |\Sigma_4| &= 0. \end{aligned}$$

This shows the second result: $\|\hat{v}_h\|_0 \leq ch \|v_h\|_{3/2}$. ■

We can summarize both lemmas in the following theorem.

Theorem 4.1 (Convergence of the 2-level scheme). *Let e_h^{m+1} be an error after one 2-level step with m damped Jacobi-smoothing steps and initial error e_h^0 . Using the grid transfer routines I_{2h}^h , and meeting Condition I, we get the error reduction*

$$\|e_h^{m+1}\|_0 \leq C\rho(m)\|e_h^0\|_0$$

where $\rho(m) = m^{-1/4}$. In addition, if Condition II is valid, we obtain

$$\|e_h^{m+1}\|_0 \leq C\rho(m)^2\|e_h^0\|_0.$$

Hence, our method is convergent if the number m of smoothing steps is large enough.

Using standard inductive arguments [1, 2, 17], we can verify the theorem.

Theorem 4.2 (Convergence of the k -level scheme with $p \geq 2$). *Performing one step of $MG(k, u_k^0, g_k)$ with m damped Jacobi-steps t we have for Condition I and m large enough*

$$\|u_k - MG(k, u_k^0, g_k)\|_0 \leq C\rho(m)\|u_k - u_k^0\|_0$$

with $\rho(m) = m^{-1/4}$. If besides Condition II is valid, then

$$\|u_k - MG(k, u_k^0, g_k)\|_0 \leq C\rho(m)^2\|u_k - u_k^0\|_0.$$

We proved some results for the W-cycle with sufficiently many smoothing steps. It seems impossible to derive by this technique analogous estimates for the V-cycle or F-cycle, or any number of smoothing steps. However, we can easily show that the method is convergent.

Theorem 4.3. *The k -level iteration is a convergent method, if the adaptive step-size control and at least one smoothing step are applied.*

Since the stiffness matrices are positive definite, the inequality holds for the error e_k^m after m smoothing steps

$$\|e_k^m\|_k \leq c_k\|e_k^0\|_k$$

with a constant $c_k = c(h_k) < 1$. Because of the step size control we have for the correction

$$\|e_k^{m+1}\|_k \leq \|e_k^m\|_k$$

and, therefore,

$$\|e_k^{m+1}\|_k \leq c_k\|e_k^0\|_k < \|e_k^0\|_k.$$

Hence, an error reduction in each iteration step is ensured but the convergence rates are not independent of the step size h_k .

In the following, we construct transfer operators $I_{2h}^h: H_{2h}^d \rightarrow H_h^d$, satisfying Condition I, and, if need be, Condition II. The natural choice analogous to scalar nonconforming finite elements [5, 18] is the L^2 -projection $I_{2h}^{h,P}$ from H_{2h}^d to H_h^d ,

$$(I_{2h}^{h,P} w_{2h}, v_h) = (w_{2h}, v_h) \quad \forall w_{2h} \in H_{2h}^d, \quad \forall v_h \in H_h^d. \quad (4.27)$$

In matrix-vector notation with coefficient vectors X_{2h} and $X_h = I_{2h}^{h,P} X_{2h}$, we can rewrite

$$M_{h,h} X_h = N_{h,2h} X_{2h}, \quad \text{respectively,} \quad X_h = M_{h,h}^{-1} N_{h,2h} X_{2h}$$

where $M_{h,h}$ is the mass matrix at level h , and $N_{h,2h}$ is the transfer matrix with coefficients

$$M_{h,h}^{(i,j)} = (v_h^{i,d}, v_h^{j,d}), \quad N_{h,2h}^{(i,j)} = (v_h^{i,d}, v_{2h}^{j,d}).$$

Lemma 4.3. *The transfer operator $I_{2h}^h = I_{2h}^{h,P}$ satisfies Conditions I and II.*

Proof. It is clear that the definition of an L^2 -projection implies

$$\|I_{2h}^h v_{2h} - v_{2h}\|_0 \leq ch \|v_{2h}\|_{2h} \quad \forall v_{2h} \in H_{2h}^d.$$

Let i_h (and analogously i_{2h}) be the standard interpolation operator $i_h: V(\Omega) \cap H^2(\Omega) \rightarrow H_h^d$ (2.12), which satisfies the estimate

$$\|v - i_h v\|_0 + h \|v - i_h v\|_h \leq ch^2 \|v\|_2 \quad \forall v \in V(\Omega) \cap H^2(\Omega).$$

Then, letting $\Pi_h = i_h$ and $\Pi_{2h} = i_{2h}$,

$$\begin{aligned} \|\Pi_h v - I_{2h}^h \Pi_{2h} v\|_0^2 &= (\Pi_h v - I_{2h}^h \Pi_{2h} v, \Pi_h v - I_{2h}^h \Pi_{2h} v) \\ &= (\Pi_h v - I_{2h}^h \Pi_{2h} v, \Pi_h v - \Pi_{2h} v) \\ &\leq \|\Pi_h v - I_{2h}^h \Pi_{2h} v\|_0 \{ \|v - \Pi_h v\|_0 + \|v - \Pi_{2h} v\|_0 \} \end{aligned}$$

and, consequently, $\|\Pi_h v - I_{2h}^h \Pi_{2h} v\|_0 \leq ch^2 \|v\|_2$.

Furthermore, using a standard inverse inequality implies

$$\|\Pi_h v - I_{2h}^h \Pi_{2h} v\|_h \leq ch^{-1} \|\Pi_h v - I_{2h}^h \Pi_{2h} v\|_0 \leq ch \|v\|_2.$$

Condition II is straightforward, since equation (1) in Condition II is just the definition, and estimate (2) is a direct consequence for L^2 -projections.

We have thus developed a grid transfer operator which is easy to analyze, and the convergence rates are also excellent. However, in each transfer step a mass matrix problem

$$M_{h,h} X_h = Y_h$$

where $Y_h = N_{h,2h} X_{2h}$, must be solved. The mass matrix corresponds to a second-order problem, and the part for the streamfunction values is equivalent to a conformingly discretized Laplacian operator [compare with (3.4)]. Consequently, we need fast Poisson solvers for each prolongation and restriction, which may be a second (standard) multigrid algorithm. However, the numerical effort is enormous. Thus we are looking for simpler transfers with about the same convergence rates. For this we present two operators which act on macroelements at level $2h$, interpolating directly into the divergence-free subspace at level h . Then, the problem is to show that the approximation properties are good enough. We consider the macrotriangle and quadrilateral with streamfunction values Ψ_i and tangential components $U_{t,j}$ (Fig. 2). One regular refinement leads to Fig. 3. We have to define three, respectively, five new streamfunction values at the vertices, and tangential components at all new edges. At vertices belonging to the macrolevel the values are retained. Then our elementwise macrointerpolation can be defined as follows:

The elementwise macrointerpolation algorithm

- (1) Transfer the divergence-free coefficient vector $(\Psi_{2h}, U_{t_{2h}})$ to the primitive coefficient vector (U_{2h}, V_{2h}) .
- (2) Interpolate 'fully' on the macro elements to get (U_h, V_h) .
- (3) Compute the tangential and normal components U_{t_h} and U_{n_h} at all fine grid edges.
- (4) Set $\Psi_h = \Psi_{2h}$ at the macro nodes and calculate at the new vertices the values for Ψ_h by integrating U_{n_h} .
- (5) Take the average for Ψ_h and U_{t_h} , which lie at macroedges.

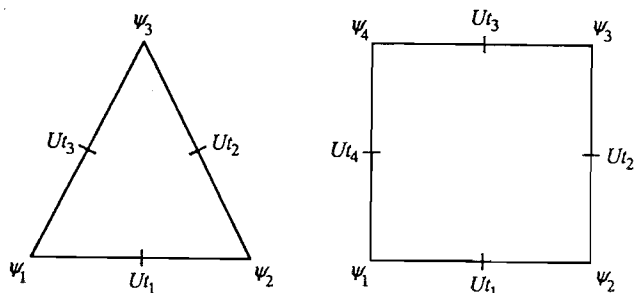


Figure 2. Macro element.

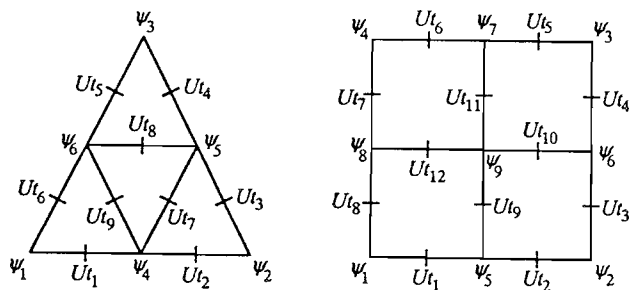


Figure 3. Refined elements.

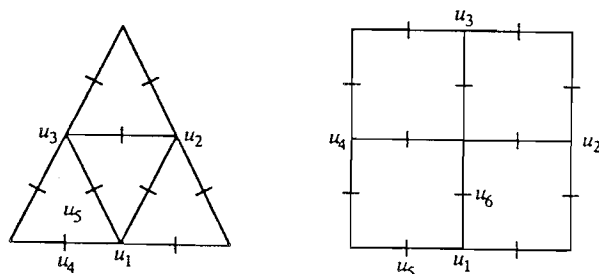


Figure 4. Configuration for interpolation.

In the following, we denote the full interpolation of the primitive nonconforming finite elements by I_{2h} . The problem to be analyzed is that the values for the inner normal velocities are only implicitly given while the tangential ones are directly defined. Let us start using the 'full' interpolation for I_{2h} , which implies linear or rotated bilinear interpolation on each macroelement. Then we get the prescriptions for the function values (Fig. 4) at the new edges [18]. For the linear case we calculate

$$u_4 = u_1 - \frac{1}{2}u_2 + \frac{1}{2}u_3, \quad u_5 = \frac{1}{2}(u_1 + u_3) \quad (4.28)$$

for the trial space $H_h^{(a)}$

$$u_5 = u_1 - \frac{1}{2}u_2 + \frac{1}{2}u_4, \quad u_6 = \frac{5}{8}u_1 + \frac{1}{8}(u_2 + u_3 + u_4) \quad (4.29)$$

and for $H_h^{(b)}$

$$u_5 = \frac{15}{16}u_1 - \frac{3}{16}u_2 - \frac{1}{16}u_3 + \frac{5}{16}u_4, \quad u_6 = \frac{9}{16}u_1 + \frac{3}{16}u_2 + \frac{1}{16}u_3 + \frac{3}{16}u_4. \quad (4.30)$$

This choice for I_{2h} is denoted by I_{2h}^L . Another possibility is to use a constant interpolation I_{2h}^K on each macro element, which results for the linear elements in

$$u_4 = u_1, \quad u_5 = u_2 \quad (4.31)$$

and for the quadrilateral spaces $H_h^{(a/b)}$

$$u_5 = u_1, \quad u_6 = u_1. \quad (4.32)$$

Before starting with the analysis, we would like to make some remarks concerning an efficient implementation. The described procedure looks very complicated, following step (1)–(5). The main idea is to rewrite this procedure using local matrices, resulting in 15×6 , respectively, 21×8 elementwise defined matrices. This has to be done very carefully but we obtain discretely divergence-free interpolation operators comparable to corresponding operators for scalar Poisson equations [16] with quadratic elements in terms of computational effort required.

For the analysis we start with the operator $I_{2h}^h = I_{2h}^{h,L}$ which is identical to the operator proposed by Brenner [2], only formulated differently. Since our quadrilateral elements are not pointwise divergence-free, we have to introduce slight modifications. However, we demonstrate this technique for the linear elements, since the analysis of the quadrilateral elements is the same but with more technical details.

In Section 3 we introduced on $H_{2h}^d \oplus H_h^d$ the inner product $(\cdot, \cdot)_{d,h}$

$$(u_h, v_h)_{d,h} := \frac{1}{3} \sum_{T \in \mathcal{T}_h} |T| \sum_{\Gamma \in \partial T} F_\Gamma(u_h) \cdot F_\Gamma(v_h) \quad (4.33)$$

and the induced norm $\|\cdot\|_{d,h}$ which in our configuration is identical to the L^2 -norm. Analogously, we can show that the elementwise defined functional $\Theta_T(v_h)$, with

$$\Theta_T(v_h) := \sum_{\Gamma, \Gamma' \in \partial T} (F_\Gamma(v_h) - F_{\Gamma'}(v_h))^2 \quad (4.34)$$

defines a norm $\|\cdot\|_{\Theta,h}$ which is equivalent to the energy norm,

$$\|v_h\|_{\Theta,h} := \left(\sum_{T \in T_h} \Theta_T(v_h) \right)^{1/2}. \quad (4.35)$$

Then, the relations are valid

$$\begin{aligned} \|v_h\|_0^2 &\sim ch^2 \sum_{T \in T_h} \sum_{\Gamma \in \partial T} |v_h(m_\Gamma)|^2 \sim ch^2 \sum_{\Gamma \subset \partial T_h} |v_h(m_\Gamma)|^2 \\ \|v_h\|_h^2 &\sim \sum_{T \in T_h} \sum_{\Gamma_i, \Gamma_j \in \partial T} |v_h(m_{\Gamma_i}) - v_h(m_{\Gamma_j})|^2. \end{aligned} \quad (4.36)$$

Lemma 4.4. For functions $v_{2h} \in H_{2h}^d$: $\|I_{2h}^h v_{2h} - v_{2h}\|_0 \leq ch \|v_{2h}\|_{2h}$.

Proof. We can first write

$$\|I_{2h}^h v_{2h} - v_{2h}\|_0^2 \leq ch^2 \sum_{T \in T_h} \sum_{\Gamma \in \partial T} |(I_{2h}^h v_{2h} - v_{2h}|_T)(m_\Gamma)|^2 = ch^2 (S_1 + S_2 + S_3 + S_4).$$

The expressions S_i are defined as

$$S_1 := \sum_m |(I_{2h}^h v_{2h} - v_{2h}|_{T_1})(m)|^2 + |(I_{2h}^h v_{2h} - v_{2h}|_{T_2})(m)|^2 \quad (4.37)$$

where m ranges over all the midpoints of T_h that belong to an inner edge in T_{2h} . The elements $T_1, T_2 \in T_{2h}$ contain m (Fig. 5). We further have

$$S_2 := \sum_m |(I_{2h}^h v_{2h} - v_{2h}|_T)(m)|^2 \quad (4.38)$$

where m ranges over all midpoints along T_h on $\partial\Omega$, and $T \in T_{2h}$ is the triangle that contains this midpoint (Fig. 5). We also have

$$S_3 := 2 \sum_m |(I_{2h}^h v_{2h} - v_{2h}|_T)(m) \cdot t_m|^2, \quad S_4 := 2 \sum_m |(I_{2h}^h v_{2h} - v_{2h}|_T)(m) \cdot n_m|^2 \quad (4.39)$$

where m ranges over all the midpoints of T_h that are inside an element $T \in T_{2h}$, and t_m , respectively, n_m are the unit vectors tangential and normal to the edge Γ , containing m (Fig. 6). We complete the proof by showing that for $I_{2h}^h = I_{2h}^{h,L}$ and ‘fully’ linear interpolation $I_{2h} = I_{2h}^L$ there holds:

$$S_i \leq c \|v_{2h}\|_{2h}^2. \quad (4.40)$$

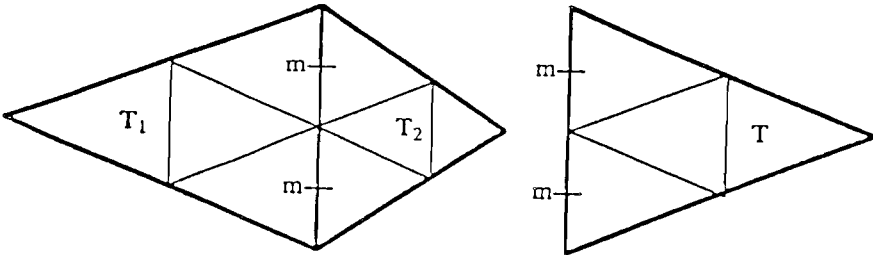
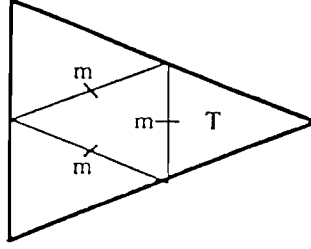
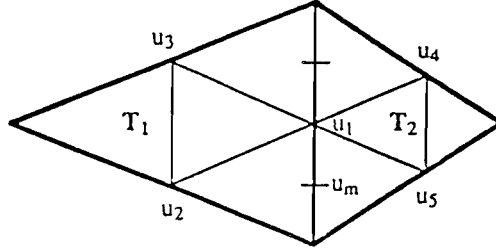


Figure 5. Figure for S_1 and S_2 .

Figure 6. Figure for S_3 and S_4 .Figure 7. Configuration for S_1 and S_2 .

We begin with S_1 and S_2 and consider the following configuration (Fig. 7). The proof in this case is analogous to that of Brenner [2]. The definitions of I_{2h}^h and I_{2h} imply:

$$\begin{aligned}
 & |(I_{2h}^h v_{2h} - v_{2h}|_{T_1})(m)|^2 + |(I_{2h}^h v_{2h} - v_{2h}|_{T_2})(m)|^2 \\
 &= \left[(u_1 + \frac{1}{4}(u_2 - u_3 + u_5 - u_4)) - (u_1 + \frac{1}{2}(u_2 - u_3)) \right]^2 \\
 &\quad + \left[(u_1 + \frac{1}{4}(u_2 - u_3 + u_5 - u_4)) - (u_1 + \frac{1}{2}(u_5 - u_4)) \right]^2 \\
 &= \left[\frac{1}{4}(u_3 - u_2) + \frac{1}{4}(u_5 - u_4) \right]^2 + \left[\frac{1}{4}(u_2 - u_3) + \frac{1}{4}(u_4 - u_5) \right]^2.
 \end{aligned}$$

Referring to the definition of $\Theta_{T_i}(v_{2h})$, we obtain

$$S_1 = \sum_m |(I_{2h}^h v_{2h} - v_{2h}|_{T_1})(m)|^2 + |(I_{2h}^h v_{2h} - v_{2h}|_{T_2})(m)|^2 \leq c \|v_{2h}\|_{2h}^2$$

$$S_2 = \sum_m |(I_{2h}^h v_{2h} - v_{2h}|_T)(m)|^2 \leq c \|v_{2h}\|_{2h}^2.$$

For S_3 there is nothing to show since by definition: $I_{2h}^h v_{2h}(m) \cdot t_m = v_{2h}(m) \cdot t_m$, and therefore, $S_3 = 0$.

The last and most interesting term is S_4 . Our problem is to determine the value for $I_{2h}^h v_{2h}(\cdot) \cdot n_m$ at the edge S_m (Fig. 8). We know

$$v_{2h}(m) \cdot n_m = u_m \cdot n_m = \frac{1}{2}(u_1 + u_3) \cdot n_m, \quad I_{2h}^h v_{2h}(m) \cdot n_m = \frac{\psi_6 - \psi_4}{|S_m|}. \quad (4.41)$$

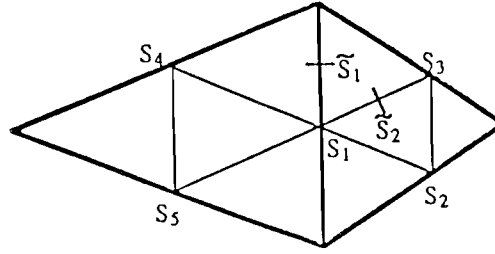


Figure 9. Figure for Lemma 4.6.

The second inequality in Condition I is proved by using homogeneity arguments. For this we need the lemma concerning estimates on the reference element. The proof can be found in [2, 17].

Lemma 4.5. *Let G be a union of two triangles T_1, T_2 with $\text{diam } G = 1$. Referring to Fig. 9, there exist constants c and C , dependent only on the angles of T_1, T_2 , such that for all functions $u \in H^2(G)$:*

$$(a) \left| \frac{1}{|S_1|} \oint_{S_1} u \, d\sigma + \frac{1}{4} \left(\frac{1}{|S_3|} \oint_{S_3} u \, d\sigma - \frac{1}{|S_2|} \oint_{S_2} u \, d\sigma + \frac{1}{|S_4|} \oint_{S_4} u \, d\sigma - \frac{1}{|S_5|} \oint_{S_5} u \, d\sigma \right) - \frac{1}{|\tilde{S}_1|} \oint_{\tilde{S}_1} u \, d\sigma \right| \leq c|u|_{H^2(G)};$$

$$(b) \left| \frac{1}{2} \left(\frac{1}{|S_1|} \oint_{S_1} u \, d\sigma + \frac{1}{|S_2|} \oint_{S_2} u \, d\sigma \right) - \frac{1}{|\tilde{S}_2|} \oint_{\tilde{S}_2} u \, d\sigma \right| \leq C|u|_{H^2(G)}.$$

To show the second relation in Condition I we again need an interpolation operator $\Pi_h: V(\Omega) \cap H^2(\Omega) \rightarrow H_h^d$, satisfying

$$\|v - \Pi_h v\|_0 + h\|v - \Pi_h v\|_h \leq ch^2\|v\|_2 \quad \forall v \in V(\Omega) \cap H^2(\Omega).$$

As before, let $\Pi_h = i_h$ be a standard interpolation operator.

Lemma 4.6. *For $v \in V(\Omega) \cap H^2(\Omega)$: $\|\Pi_h v - I_{2h}^h \Pi_{2h} v\|_0 \leq ch^2\|v\|_2$.*

Proof. As before we make the splitting

$$\begin{aligned} \|\Pi_h v - I_{2h}^h \Pi_{2h} v\|_0^2 &\leq ch^2 \sum_{T \in \mathcal{T}_h} \sum_{\Gamma \in \partial T} |\Pi_h v - I_{2h}^h \Pi_{2h} v|(m_\Gamma)|^2 \\ &= ch^2(S_1 + S_2 + S_3 + S_4). \end{aligned}$$

Lemma 4.5 and standard estimates for finite elements (see, for instance, [6]) lead to

$$S_1 + S_2 + S_3 \leq ch^2\|v\|_2^2.$$

Since $\Pi_h v - I_{2h}^h \Pi_{2h} v \in H_h^d$ is discretely divergence-free, we also have

$$S_4 \leq c(|S_1| + |S_2|) \leq ch^2\|v\|_2^2$$

which implies the desired result. ■

With analogous conclusions, the proof of which requires more technical details due to a larger number of local degrees of freedom Condition I can be shown for the quadrilateral cases. Condition II could not be proved for this operator, only for the choice $I_{2h}^h = I_{2h}^{h,P}$.

For the operator $I_{2h}^h = I_{2h}^{h,K}$ which is a modification of $I_{2h}^{h,L}$, using the locally constant interpolation operator I_{2h}^K , we can only show a slightly weaker result [16].

Lemma 4.7. *The inequality holds:*

$$\|I_{2h}^h v_{2h} - v_{2h}\|_0 \leq ch \|v_{2h}\|_{2h} \quad \forall v_{2h} \in H_{2h}^d.$$

We have not proved the second relation for I_{2h}^K ,

$$\|\Pi_h v - I_{2h}^h \Pi_{2h} v\|_0 + h \|\Pi_h v - I_{2h}^h \Pi_{2h} v\|_h \leq ch^2 \|v\|_2 \quad \forall v \in V(\Omega) \cap H^2(\Omega). \quad (4.42)$$

Nevertheless, this operator is one of those used in our test calculations. There is another approach for developing $I_{2h}^{h,K}$. We consider the discretization of the generalized Stokes problem

$$\alpha u - \varepsilon \Delta u + \nabla p = f, \quad \nabla \cdot u = 0 \quad (4.43)$$

with $\alpha > 0$, $\varepsilon \geq 0$. As $\varepsilon \rightarrow 0$, the effect of the Stokes operator decreases, and for $\varepsilon = 0$, we only have to solve a linear system for the mass matrix $M_{h,h}$. As mentioned above, the streamfunction part of this matrix is spectrally equivalent to the Laplacian matrix which is discretized using conforming linear or bilinear finite elements. Hence, it seems logical to solve this system by conforming multigrid routines. This procedure, however, is exactly the same as the one proposed for $I_{2h}^{h,K}$, if for the tangential part at the edges the operator I_{2h}^K is taken. In the subsequent section we carefully examine the numerical cost of solving the Stokes equations by the different schemes proposed.

Table 1. Rates for grid I.

	κ			γ		
NEQ =	3201	12545	49665	3201	12545	49665
$I_{2h}^{h,K}$						
GS1	0.404	0.834	1.220	0.714	3.440	—
GS2	0.193	0.210	0.298	0.597	0.612	0.840
GS4	0.161	0.162	0.165	0.815	0.808	0.849
$I_{2h}^{h,L}$						
GS1	0.128	0.118	0.111	0.544	0.473	0.467
GS2	0.104	0.092	0.106	0.622	0.548	0.619
GS4	0.082	0.078	0.078	0.775	0.718	0.801
$I_{2h}^{h,P}$						
GS1	0.139	0.144	0.147	1.220	1.180	1.620
GS2	0.066	0.058	0.050	1.080	1.010	1.250
GS4	0.057	0.054	0.048	1.230	1.210	1.730

Table 2. Rates for grid II.

	κ			γ		
$NEQ =$	2417	9441	37313	2417	9441	37313
$I_{2h}^{h,K}$						
GS1	0.434	0.764	1.130	0.708	2.370	—
GS2	0.356	0.379	0.440	0.856	0.947	1.200
GS4	0.264	0.302	0.327	1.010	1.240	1.550
$I_{2h}^{h,L}$						
GS1	0.190	0.184	0.186	0.591	0.600	0.698
GS2	0.136	0.143	0.143	0.605	0.667	0.792
GS4	0.099	0.119	0.118	0.730	0.865	1.010
$I_{2h}^{h,P}$						
GS1	0.241	0.254	0.275	2.040	2.060	3.120
GS2	0.175	0.196	0.220	1.880	1.940	2.890
GS4	0.123	0.148	0.173	1.770	1.930	2.930

Table 3. Rates for grid III.

	κ			γ		
$NEQ =$	2433	9473	37377	2433	9473	37377
$I_{2h}^{h,K}$						
GS1	0.661	1.320	1.430	1.780	—	—
GS2	0.286	0.321	0.545	0.811	0.998	1.950
GS4	0.212	0.229	0.249	1.060	1.250	1.370
$I_{2h}^{h,L}$						
GS1	0.237	0.246	0.259	0.957	1.040	1.120
GS2	0.175	0.193	0.211	0.964	1.100	1.200
GS4	0.144	0.136	0.155	1.190	1.280	1.440
$I_{2h}^{h,P}$						
GS1	0.254	0.283	0.307	4.910	5.100	6.640
GS2	0.151	0.184	0.210	3.660	3.980	5.250
GS4	0.091	0.119	0.141	3.070	3.530	4.450

Table 4. Rates for ellipse.

	κ			γ	
$NEQ =$	5184	20352		5184	20352
$I_{2h}^{h,K}$					
GS2	2.450	4.840	—	—	—
GS4	1.880	3.120	—	—	—
GS8	1.030	1.970	—	—	—
GS16	0.473	0.981	16.00	36.50	—
$I_{2h}^{h,L}$					
GS2	0.282	0.276	3.450	2.500	—
GS4	0.153	0.141	2.960	2.420	—

Table 5. Grid I with $I_{2h}^{h,K}$ and $\alpha = 10^n$, $n = 0, 3, 6, 9$.

		κ			γ		
n		3201	12545	49665	3201	12545	49665
0	GS1	0.473	0.800	1.290	0.665	2.468	—
	GS2	0.195	0.193	0.292	0.470	0.483	0.657
3	GS1	0.286	0.325	0.419	0.435	0.490	0.645
	GS2	0.173	0.170	0.180	0.434	0.450	0.470
6	GS1	0.028	0.025	0.082	0.154	0.150	0.225
	GS2	0.015	0.023	0.083	0.182	0.211	0.325
9	GS1	0.020	0.025	0.030	0.140	0.150	0.160
	GS2	0.020	0.019	0.017	0.197	0.198	0.197

5. NUMERICAL RESULTS

Our aim is to examine the influence of different smoothing and transfer operators and different meshes on the efficiency and robustness of our multigrid algorithm. As a smoothing operator, we restrict ourselves to the Gauß–Seidel method which is about as expensive as the Jacobi-iteration, at least on scalar workstations like the SUN 4/260 used. The case of the ILU-method is studied in [19], in which we give an overview of possible renumbering strategies. For the grid transfer routines we expect that the projection method $I_{2h}^{h,P}$ will have the best convergence rates followed by $I_{2h}^{h,L}$ and $I_{2h}^{h,K}$. But these convergence rates are not a true measure since, for instance, Gaussian elimination has the best rates, namely zero. In order to take account of this discrepancy we introduce efficiency rates as a measure in real time.

We start with the standard problem of the Stokes Driven Cavity on a unit square,

$$\begin{aligned}\Delta u - \nabla p &= 0, & \nabla \cdot u &= 0 \quad \text{in } \Omega \\ u &= 0 \quad \text{on } \partial\Omega \setminus \{y = 1\}, & u &= (1, 0)^T \quad \text{on } \partial\Omega \cap \{y = 1\}\end{aligned}$$

with the coarse grids as typical representations of possible meshes (Fig. 10). The finer subdivisions are generated using the regular refinement process as described in Section 2. In the tables we present the number of unknowns (NEQ), the number m of pre- and postsmoothing steps, the convergence rate κ and the efficiency rate γ ,

$$\kappa = \sqrt[8]{|r^{(8)}|/|r^{(0)}|}, \quad \gamma = -\frac{1000T_8}{8NEQ \log \kappa}. \quad (5.1)$$

Here, $r^{(8)}$ denotes the residual after 8 iterations, and T_8 the corresponding computational time. The efficiency rate γ measures the time in milliseconds needed to gain one digit per unknown. For the operator $I_{2h}^{h,L}$ we used the adaptive step length control, while for $I_{2h}^{h,K}$ a fixed value smaller than 1, and for $I_{2h}^{h,P}$ the choice $\alpha = 1$, due to the character of a projection method, seems optimal. The numbers are generated using an F-cycle, since the V-cycle seems unstable sometimes, while the W-cycle shows no visible advantages. As finite element space, we use the space $H_h = H_h^{(b)}$. The tables show that the projection method leads to the best convergence rates but at the expense of the greatest computational effort. The constant operator $I_{2h}^{h,K}$ leads to surprisingly good results, but the robustness against grid irregularities seems to be lost, at least as compared to $I_{2h}^{h,L}$, which produces the best results. Similar results can be obtained in the next domain, which simulates the flow around an ellipse. This is a practical example of domains (a coarse grid, see Fig. 11) as to concerning the Navier-Stokes equations. As a final example, we show the results for the class of problems (with $\alpha \geq 0$)

$$\alpha u - \Delta u + \nabla p = f, \quad \nabla \cdot u = 0. \quad (5.2)$$

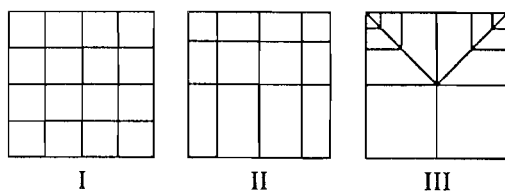


Figure 10. Used coarse grids.

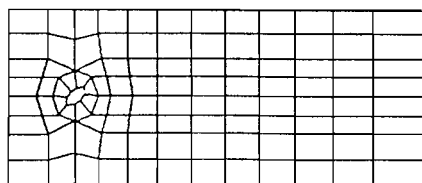


Figure 11. Coarse grid for ellipse configuration.

This configuration is a typical example for an unsteady calculation, where the mass matrix is weighted with $O(1/\Delta t)$. Here, the values $\alpha = 10^n$, $n = 0, 3, 6, 9$, are taken. Our theoretical considerations as to the influence as $\alpha \rightarrow \infty$ are justified. $I_{2h}^{h,K}$ is now the best but our favourite $I_{2h}^{h,L}$ was not much worse, only the projection method was surprisingly bad.

Summarizing, we have found an interpolation operator, namely $I_{2h}^{h,L}$, which satisfies all requirements: small numerical effort, good convergence rates, robust against grid and parameter variations, and theoretically analyzable. In connection with the Gauß-Seidel iteration as a smoother in our algorithm, we seem to have found a good candidate as a Black Box solver for linear systems in a fully nonstationary Navier-Stokes code [16–18].

REFERENCES

1. R. E. Bank and T. Dupont, An optimal order process for solving finite element equations. *Math. Comp.* (1981) 36, 35–51.
2. S. C. Brenner, A nonconforming multigrid method for the stationary Stokes equations. *Math. Comp.* (1990) 55, 411–437.
3. S. C. Brenner, An optimal order multigrid method for P1 nonconforming finite elements. *Math. Comp.* (1989) 52, 1–15.
4. S. C. Brenner, An optimal order nonconforming multigrid method for the biharmonic equation, *SIAM J. Numer. Anal.* (1989) 26, 1124–1138.
5. D. Braess and R. Verfürth, Multi-grid methods for non-conforming finite element methods. *Technical report No. 453*, SFB 123, University Heidelberg, 1988.
6. Ph. G. Ciarlet, *The Finite Element Method for Elliptic Problems*. North-Holland, 1976.
7. M. Crouzeix and P. A. Raviart, Conforming and non-conforming finite element methods for solving the stationary Stokes equations. *R.A.I.R.O.* (1973) R-3, 77–104.
8. C. Cuvelier, A. Segal, and A. Steenhoven, *Finite element methods and Navier Stokes equations*. D. Reidel Publishing Company, Dordrecht, 1986.
9. V. Girault and P. A. Raviart, *Finite Element Methods for Navier-Stokes equations*. Springer, Berlin-Heidelberg, 1986.
10. D. Griffiths, An approximately divergence-free 9-node velocity element (with variations) for incompressible flows. *Int. J. Num. Meth. Fluids* (1981) 1, 323–346.
11. W. Hackbusch, *Multi-Grid Methods and Applications*. Springer, Berlin-Heidelberg, 1985.
12. L. S. D. Morley, The triangular equilibrium problem in the solution of plate bending problems. *Aero. Quart.* (1968) 19, 149–169.
13. P. Peisker, Zwei numerische Verfahren zur Lösung der biharmonischen Gleichung unter besonderer Berücksichtigung der Mehrgitteridee. *Thesis*, University of Bochum, 1985.
14. R. Rannacher and S. Turek, A simple nonconforming quadrilateral Stokes element. *Numer. Meth. Part. Diff. Eq.* (1992) 8, 97–111.
15. F. Thomasset, *Implementation of Finite Element Methods for Navier-Stokes Equations*. Springer, New York 1981.
16. S. Turek, Ein robustes und effizientes Mehrgitterverfahren zur Lösung der instationären, inkompressiblen 2-D Navier-Stokes-Gleichungen mit diskret divergenzfreien finiten elementen. *Thesis*, University of Heidelberg, 1991.
17. S. Turek, Tools for simulating non-stationary incompressible flow via discretely divergence-free finite element models. *Int. J. Num. Meth. Fluids* (1994) 18, 71–107.
18. S. Turek, Mehrgitterverfahren für eine Klasse von nichtkonformen Finite Elemente Diskretisierungen, *Diploma Thesis*, Saarbrücken, 1988.
19. S. Turek, On ordering strategies in a multigrid algorithm. In: *Proc. 8th GAMM-Seminar, Kiel, January 24–26, 1992, Notes on Numerical Fluid Mechanics*. Volume 41, Vieweg, Braunschweig, 1993.